

Development of a Diamond Radiation Detector using Boron-Doped Layer as a Neutron Converter

Tomoaki Masuzawa¹, and Takatoshi Yamada²

masuzawa.tomoaki@shizuoka.ac.jp, takatoshi-yamada@aist.go.jp

¹Research Institute of Electronics, Shizuoka University, 3-5-1 Naka-ku, Johoku, Hamamatsu 432-8011 Japan

²Nano Carbon Device Research Center, National Institute of Advanced Industrial Science and Technology(AIST), 1-1-1 Higashi Tsukuba 305-8565 Japan

Keywords: diamond; radiation detector; neutron; boron-doped

ABSTRACT

A radiation detector made of boron(B)-doped/undoped diamond film stacking structure has been proposed, aiming at neutron detection using B-doped layer as a neutron-alpha converter. A prototype detector was fabricated using chemical vapor deposition (CVD)-grown polycrystalline diamond, and detections of both alpha particle and neutron were demonstrated. In addition, detection of alpha particle was characterized to investigate carrier transport and band model of the detector operation. The results indicate that improvement of charge collection in the polycrystalline diamond is the key to improve the sensitivity of the detector.

1 Introduction

Diamond is a wide bandgap semiconductor having high carrier mobility and long carrier lifetime[1,2]. Although high sensitivity radiation detectors were reported using single-crystal diamonds[3-5], typical size with a few mm of single crystalline diamond is one of the remaining issues for radiation image sensors. Polycrystalline diamond films can be deposited in large size by CVD[6,7], however it is considered that grain boundaries prevent the superior electrical properties of diamond.

In this study, radiation detection characteristics of polycrystalline diamond were evaluated by using neutron and alpha-particle measurements. In order to detect neutrons, which do not have electrical charges, a boron(B)-doped diamond layer was introduced as a neutron-alpha particle converter: a stacking structure of B-doped converter layer (~2μm) and thick (> 40μm) undoped layer, where high electrical field could be applied to collect carriers, was proposed as a possible detector structure[8].

Detection of neutrons was modeled as follows: first, the incident neutrons were captured by ¹⁰B in the B-doped diamond layer, and alpha particles were generated by ¹⁰B(n, α)⁷Li reaction. Second, the alpha particles were scattered in the diamond films and generated signal carriers, which conducted through undoped layer and were detected as signal charges. Detection of neutron and alpha particles were demonstrated using californium (Cf)-252 and americium (Am)-241 radioactive isotopes for neutron and alpha-particle sources. The radiation detection characteristics were analyzed to investigate

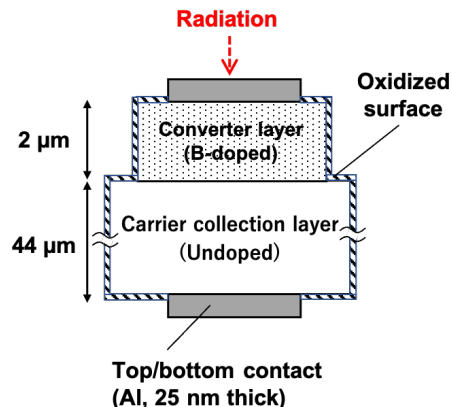


Fig. 1 Detector structure [8]

carrier transport property in the polycrystalline diamond detectors.

2 Experiment

A prototype 1-pixel detector was fabricated, which consisted of stacking B-doped and undoped polycrystalline diamond layers. Fig. 1 illustrates the detector structure.

2.1 Detector fabrication

B-doped and undoped polycrystalline diamond films were grown by hot-filament(HF) CVD technique[8], using the setup illustrated in Fig. 2. A tungsten filament was fixed above the substrate, and was heated up to 2300 °C. Gaseous hydrogen (H₂) and methane (CH₄) were supplied to the reaction chamber via mass-flow

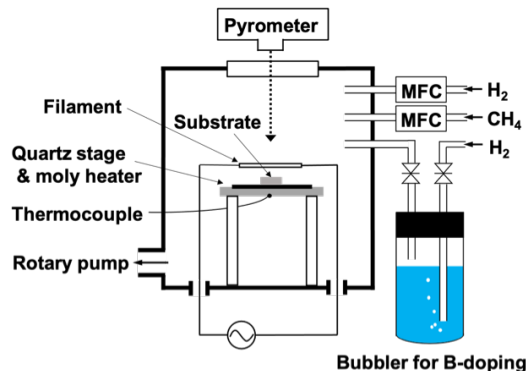


Fig. 2 Schematic diagram of HFCVD system

controllers, while the chamber was evacuated to a total pressure of 100 Torr. The system was equipped with a bubbling system for B-doping. Typical growth rate was approximately 1 $\mu\text{m}/\text{h}$.

First, undoped thick-film ($>40\mu\text{m}$) diamond was grown on Si(100) substrates, and the Si substrates were removed by wet chemical etching to obtain free-standing diamond films. Typical thickness of the undoped diamond film was approximately 44 μm . Then, B-doped diamond layer was grown on the undoped diamond self-standing film to serve as a neutron converter. The boron source was trimethyl borate (TMB) dissolved in acetone. The source gas was introduced into the chamber by bubbling using H_2 as a carrier gas. The B/C ratio in the source gas was calculated to be 1%. B-doped diamond films were grown for 2 h with a typical thickness of 2 μm . In this study, Si surface was processed with ultrasonication in a detonation nanodiamond dispersed solution to increase diamond nucleation [9].

The surface morphology of the diamond film was observed by scanning electron microscopy (SEM) as shown in Fig. 3 and average grain size of polycrystalline surface was about 200 nm. Crystal structure of the B-doped diamond film was characterized using confocal Raman spectroscopy. Laser wave-length and power were 532 nm and 11 mW, respectively. The spot size of the laser was about 1 μm . Typical Raman spectrum, shown in Fig. 4, indicates a strong sharp peak of diamond at 1333 cm^{-1} and a broad peak at around 1550 cm^{-1} due to amorphous/non-diamond components, which were considered to be from grain boundaries.

Boron content in the diamond films were estimated by time-of-flight secondary ion mass spectroscopy (TOF-SIMS). Measurement conditions were as follows: primary ion beam was Bi^+ at 25 kV, 2.0 pA, and sputter beam was Cs^+ at 2 kV, 100 nA, respectively. Field of view was approximately $20 \times 20 \mu\text{m}$. Fig. 5 shows TOF-SIMS profiles of a B-doped/undoped diamond stacking structure. It was confirmed that boron existed in the film by CB^- ion signals and B-doped/undoped diamond stacking structure was obtained. It should be noted that absolute boron concentration cannot be determined. In addition, x-ray photoelectron spectroscopy (XPS) using monochromatic $\text{Al K}\alpha$ (1487 eV) was used to evaluate boron doping in diamond films[8]. Despite the detection limit of XPS (0.1 mol%), B1s peak was observed by the XPS. In addition, peak area analysis also suggests that the B concentration in the B-doped layer in B-doped/undoped stacking structure was approximately 0.1%, which is in the order of 10^{20}cm^{-3} .

Aluminum (Al) Schottky electrodes were deposited on both B-doped and undoped diamond surfaces (Fig.1) by thermal evaporation. Thickness of Al contacts were 25 nm. The thickness was designed to allow alpha particles to be introduced to the detector through the electrode.

In order to remove conductive layer on diamond surface, oxidization was carried out [10]. The detector structure was placed in a quartz tube and annealed at 450 $^\circ\text{C}$ in mixed N_2 and O_2 gas (4:1) for 1 h.

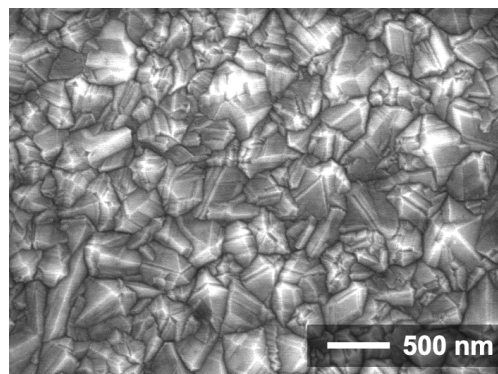


Fig. 3 SEM image of polycrystalline CVD diamond [8]

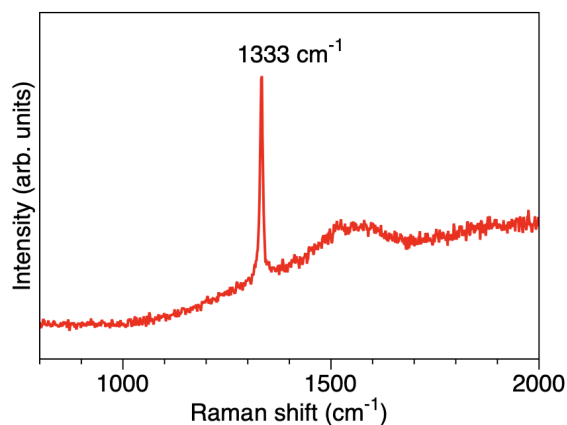


Fig. 4 Raman spectrum of B-doped/Undoped stacked polycrystalline diamond

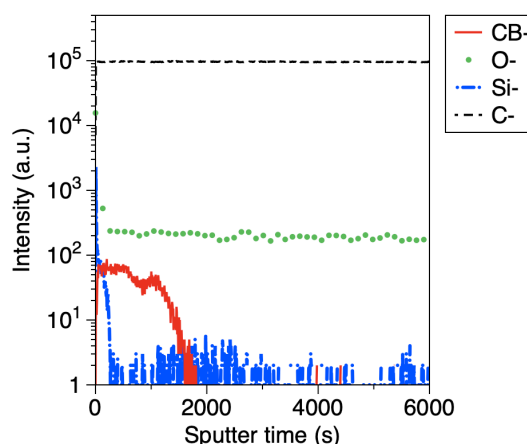


Fig. 5 TOF-SIMS spectrum of B-doped/Undoped polycrystalline diamond stacked structure

2.2 Radiation detection

The diamond radiation detector was designed to detect neutrons and alpha particles. The B-doped layer works as a neutron-alpha converter through the $^{10}\text{B}(n, \alpha)^7\text{Li}$ reaction. The undoped layer has high resistivity and acts as a carrier collection layer. To detect radiation signal, the detector was connected to a preamplifier (charge amplifier) and a multi-channel analyzer (MCA) to count the pulse signals generated by incident (or converted) alpha particles. Fig. 6 shows a schematic diagram of the circuit for radiation measurement.

Neutron and alpha-particle detection were conducted using Cf-252 as a neutron source, and Am-241 as an alpha-particle source. The radioactivity of the Cf and Am were 1.4×10^6 Bq, and 3.9×10^6 Bq, respectively.

For neutron detection, the radiation detector was connected to a preamplifier and MCA, and Cf was placed at 70 mm from the detector. Both the detector and RI were surrounded with paraffin blocks. The paraffin blocks were also placed between the Cf and the detector for neutron moderator, where incident neutrons were decelerated to thermal neutrons with kinetic energy of ~ 25 meV.

Alpha-particle detection was carried out using Am-241 alpha-particle source. The detector and the Am were placed at varied distances inside an Al shielded box. The Am-241 emits both alpha particles (5.5 MeV) and γ -rays (60 keV). A lead collimator (1 mm diameter) was inserted between Am and the detector to limit the incident angle. The alpha particles were introduced to the detector on the B-doped side through an Al contact.

3 Results and Discussion

Fig. 7 shows a typical neutron signal obtained using diamond detector. The x-axis of the Fig. 7 is channel number of MCA, which represents pulse height of the radiation signals. The higher incident radiation energy is, the more signal pulses are detected, which is counted for higher pulse height. Therefore, the x-axis of the MCA virtually represents a radiation energy.

In Fig. 7, a broad peak at around 800 ch as well as a shoulder at 300-700 ch were observed. The broad peak at 800 ch originate in alpha particles converted by neutron capture reaction of boron. Since the alpha particles lost their kinetic energy by multiple scatterings in the diamond film, they generate signal pulses at various pulse heights, and the spectra obtained by MCA shows a broad peak. It was considered that the shoulder-like feature at lower channel side originated from carriers scattered multiple times and lost their energy in the diamond detector. Neither the broad peak at 800 ch, nor the shoulder-like feature at 300-700 ch were observed by a measurement using undoped polycrystalline diamond without B-doped layer as a detector[8]. The results showed that neutron was successfully detected with polycrystalline diamond by using B-doped/undoped stacking structure.

Fig. 8 shows alpha-particle signal using Am-241 alpha-

particle source and B-doped/undoped stacking polycrystalline diamond detector. The source-detector distance was varied to control incident alpha-particle energy. Broad peaks were observed, and the peak energy shifted as the incident energy was varied. The results indicates that the detected broad peaks were alpha-particle signals.

Fig. 9 shows some alpha-particle signals taken under various detector bias voltages. Here, source-detector distance was fixed at 8 mm. The peak position shifted

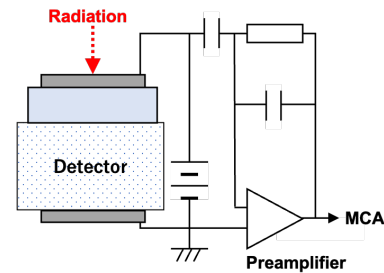


Fig. 6 Schematic circuit configuration of diamond detector[8]

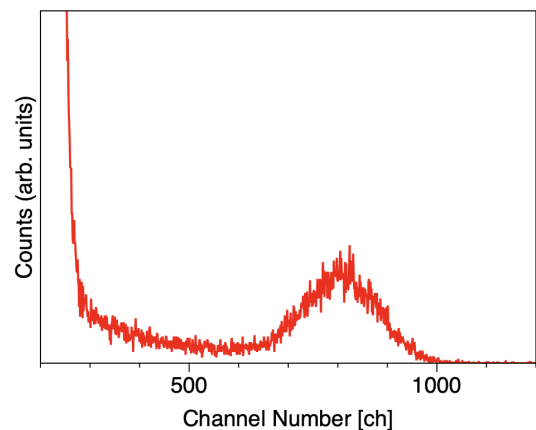


Fig. 7 Neutron signal taken with diamond detector [8]

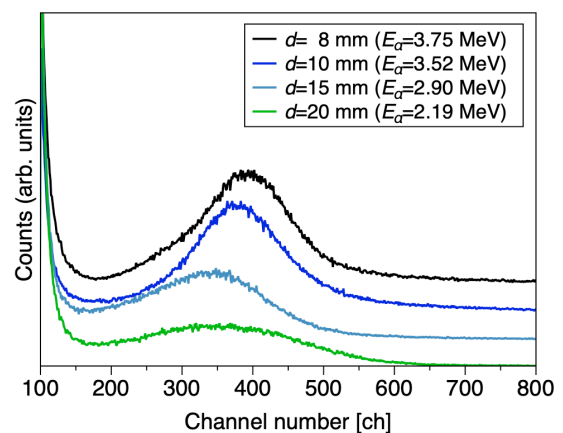


Fig. 8 Alpha-particle signal with different source-detector distances[8]

proportionally to the detector bias, as shown in Fig. 10. Shift of the peak position in the high channel-number side means that by increasing bias voltage, more signal charges are collected for the same input radiation. The more signal charges are collected, the higher the signal pulse height, and the signal is counted at higher channel number.

The results in Fig. 10 indicate that the carrier collection efficiency depends on the average electric field across the detector due to charge loss in the polycrystalline diamond. The peak shift would not be observed in single crystal diamond detectors, which had charge collection efficiency near 100%, i.e. signal charges generated in the detector were read-out without loss in the detector. In such case, the radiation peak appears at a fixed position.

The results suggested that although carrier collection efficiency of polycrystalline diamond detector is not as high as single crystal diamonds, it can still be used to detect neutrons. In our previous study [11], it was reported that an interface between B-doped diamond and undoped diamond was contributed to sensitivity for neutron detection. Further improvement of sensitivity would be expected by optimizing the boron concentration, film thickness and contact electrode on B-doped diamond.

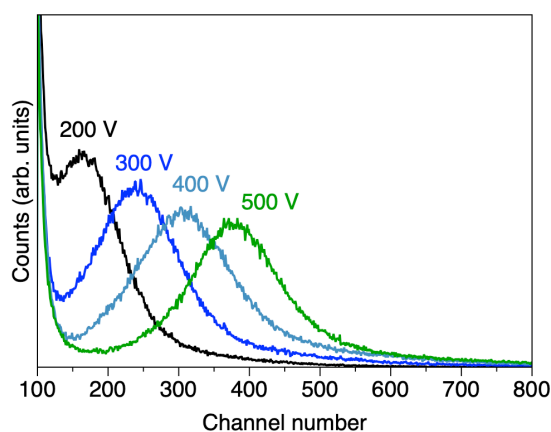


Fig. 9 Alpha-particle signals for various bias conditions

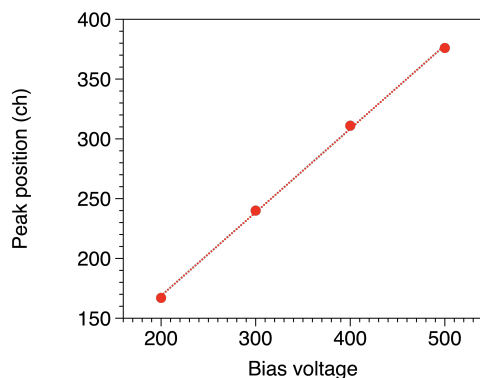


Fig. 10 Peak shift vs bias voltage derived from results in Fig. 9

4 Conclusions

Radiation detection characteristics of polycrystalline diamond were evaluated. A prototype radiation detector, which consisted of B-doped neutron converter layer and undoped carrier collection layer, was fabricated by HFCVD. Neutrons from RI were used as test input, and successful neutron detection was demonstrated using the B-doped/undoped stacking structure. In addition, Detection characteristics of alpha particles suggested that charge collection efficiency of the detector increased proportionally to the average electric field across the detector, which suggested a carrier loss in the polycrystalline diamond detector.

Acknowledgments

The authors would like to thank Prof. Hidenori Mimura, Prof. Toru Aoki, and Prof. Takayuki Nakano at Shizuoka University, for their advices and fruitful discussions on radiation detection experiments. The authors would like to thank Dr. Katsuyuki Takagi, Dr. Taku Miyake and Dr. Hisaya Nakagawa for their invaluable support on detector instrumentation.

This research is supported by grants-in-aid (20K14776, 20K21136 and 23K03939) from the Ministry of Education, Culture, Sports, Science and Technology (MEXT), Japan. This study was supported by the Research Center for Biomedical Engineering. Part of this research is conducted using the experimental facility of Hamamatsu Campus Center for Instrumental Analysis, Shizuoka University.

REFERENCES

- [1] H. Pernegger et al., *J. Appl. Phys.* 97 (2005) 073704.
- [2] L. S. Pan, D. R. Kania (Eds.): *Diamond: Electronic Properties and Applications*, Springer, 1995.
- [3] T. Behnke et al., *Nucl. Instrum. Methods Phys. Res. A* 489 (2002) 230.
- [4] Y. Sato et al., *Nucl. Instrum. Methods Phys. Res. A* 784 (2015) 147.
- [5] I. Zamboni et al., *Diam. Relat. Mater.* 31 (2013) 65.
- [6] J.H. Kaneko, et al., *Nucl. Inst. Methods Phys. Res. A* 505 (2003) 187.
- [7] P. Bergonzo, et al., *Diam. Relat. Mater.* 10 (2001) 631.
- [8] T. Miyake et al., *Physica Status Solidi A* 219 (2022) 2100315.
- [9] H. Kawarada, *Surf. Sci. Reports*, 26 (1996) 205.
- [10] M. Ozawa et al., *Adv. Mater.* 19, (2007) 1201.
- [11] T. Masuzawa et al., *Diam. Relat. Mater.* 136 (2023) 109985.